Phase Relation Studies in the CeO_2-Sm_2O_3 System at 1500 to 600 °C in Air

Andrievskaya ER, Kornienko OA* and Yurchenko Yu V

Frantsevich Institute for Materials Science Problems NAS, Ukraine

Abstract

Materials based on CeO_2-Sm_2O_3 system are promising candidates for a wide range of applications, but the phase relationship has not been studied systematically previously. To address this challenge, the subsection of the phase diagram for 600, 1100 and 1500 °C has been elucidated. Samples of different compositions have been prepared from nitrate acid solutions using conventional ceramic techniques; evaporation, drying, and calcinations. The phase relations in the binary CeO_2-Sm_2O_3 system at 600-1500 °C in air were studied from the heat treated samples using X-ray diffraction analysis and in the overall concentration range. It was established that in the binary CeO_2-$Sm_2$03 system there exist fields of solid solutions based on monoclinic (B) modification of Sm_2O_3, cubic (C) modification of Sm_2O_3 and cubic modification of CeO_2 with fluorite-type structure (F). The systematic study that covered whole composition range excluded formation of new phases. The refined lattice parameters of the unit cells and the boundaries of the homogeneity fields for solid solutions were determined.

Keywords: Phase equilibria; Ceria; Samaria; Solid solutions; Lattice parameters

ISSN: 2576-8840

***Corresponding author:** Kornienko OA, Frantsevich Institute for Materials Science Problems NAS, Ukraine

Submission: January 20, 2020

Published: February 03, 2020

Volume 12 - Issue 4

How to cite this article: Andrievskaya ER, Kornienko OA, Yurchenko Yu V. Phase Relation Studies in the CeO_2-Sm_2O_3 System at 1500 to 600 °C in Air. Res Dev Material Sci. 12(4).RDMS.000795.2020.
DOI: 10.31031/RDMS.2020.12.000795

Introduction

For many years, CeO_2-based materials have been mainly used as catalysts and pigments in ceramics or glasses. Today ceria based materials are of great worldwide interest for many engineering applications such as catalysts, solid electrolytes, laser media, radio wave absorbers, components for electronics, and so on. Much attention is now focused on development of alternative power sources which are based on electrochemical devices, in particular on fuel cells. As solid electrolytes for fuel cells that operate at high temperatures (up to 1000 °C), materials on the basis of Y_2O_3 stabilized zirconia are used, whereas ceria based solid solutions are promising as electrolytes operating at moderate temperatures (to 600 °C) [1-10].

The right choice of an optimal electrolyte depends on reliability of data on solubility limits for REE oxides in the crystalline lattice of CeO_2, since high ion conductivity corresponds to maximal concentration of compensating oxygen vacancies. This, in its turn, requires good knowledge of phase equilibria in multicomponent oxide systems. Investigations of peculiarities of REE polymorphism, exsolution and formation of ordered phases as well as of the effect of electronic structure and relations between ion radii of lanthanides on the phase transformation, structure, and stability are also of keen scientific interest. Development of new materials and technologies based on CeO_2-Ln_2O_3 solid solutions needs phase equilibria studies and knowledge of properties of the phases formed in the systems. Phase equilibria in the CeO_2 based systems added with REE oxides and properties have been partially studied [11-17].

Phase reactions in CeO_2-Sm_2O_3 system were studied in [16]. They found stable solid solutions based on cubic modification of F-CeO_2 in concentrations range from pure CeO_2 to 40 mol % Sm_2O_3 and cubic modification of C-Sm_2O_3 in the range from 50 to 90mol % Sm_2O_3 at 1400 **°C**. The lattice parameter of the unit cell of solid solutions varies from a=0.5411nm in pure CeO_2 to a=0.5452nm in the composition containing 40mol % Sm_2O_3 and from a=1.0914nm the composition containing 50mol % Sm_2O_3 to a=1.0928nm the two-phase composition (B+C) containing 90mol % Sm_2O_3. The two-phase region (F+C) in the system has not been determined correctly. The phase diagram has not been built [16].

Experimental

Cerium oxide nitrate, $Ce(NO_3)_3{\cdot}6H_2O$, samarium oxide, Sm_2O_3 (all 99.99 % produced by Merck Corp.) and analytical-grade nitric acid were used as the starting materials. In totally 24 compositions in CeO_2-Sm_2O_3 system were prepared in the present work for experimental analysis. The specimens were prepared in step 1-5mol % Sm_2O_3 as follows: mixing the cerium and samarium nitrate solutions followed by their co-evaporation and calcination at 1000 °C for 2h until uniform mixtures of oxides formed. The as-prepared powders were pressed at 10MPa into pellets of 5mm in diameter and 4mm in height. To study phase relationships at 1500 °C thermal treatment of as-prepared samples was carried out in two stages: at 1100 °C (for 846h in air) and then at 1500 °C (for 150h in air) in the furnaces with heating elements based on Fecral (H23U5T) and Superkanthal ($MoSi_2$), respectively. The two-step annealing allows removing residuals of nitrogen oxides from the samples. At lower temperatures,≤1250 °C, phase equilibria (which include processes of disordering/ordering) were reached rather slowly because of low velocity of diffusion processes in the cation sublattice, which requires long-term annealing of samples [18]. To study phase equilibria at 1100 °C and 600 °C, the heat treatment of the samples was carried out in air for 10813 hours and 33000 hours, in respectively. The heating rate was 3.5 $°C\ min^{-1}$. The cooling rate was about 100 °C/min when switching off the power from the furnace. No phase composition changes were fixed at this rate or faster cooling. This technology of preparation doesn't influence the valence of rear earth elements.

XRD analysis of samples was performed by powder procedure on a DRON-3 apparatus at ambient temperature under CuKα radiation. Scanning step was 0.05-0.1 ° in the range 2θ=15-90 °. Lattice parameters were calculated by the least square method using the LATTIC computer code with an error of not lower than 0.0001nm for the cubic phase. The phase composition was determined using the "Match" program, which utilizes PDF-2 database of standard X-ray data. Diffraction peaks parameters determined by approximating the peaks of experimental diffractograms using the Voigt function, were used for the phase identification and calculations of lattice parameters.

Results and discussion

The solid-phase reaction between CeO_2 (fluorite-type, F, space group $Fm\overline{3}m$ and Sm_2O_3 (monoclinic modification of rare-earth oxides, type B, space group C2/m) was studied at temperatures 600 °C, 1100 °C and 1500 °C. The x-ray analysis showed that three solid solutions of substitution type exist in the CeO_2-Sm_2O_3 system in the given temperature interval. Two of them have cubic symmetry (fluorite F-CeO_2 type and C-Sm_2O_3 type) and the third one has monoclinic symmetry (B-Eu_2O_3 type). The phases were separated by two-phase fields (C+F; B+C) as shown in Figure 1. Tables 1-3 contain data on the initial chemical and phase composition of samples annealed at 1500, 1100, and 600 °C as well as on lattice parameters for phases that are in equilibrium at the corresponding temperatures. Figure 2 demonstrate concentration dependences of solid solutions based on F-CeO_2 and C-Sm_2O_3 in the CeO_2-Sm_2O_3 system after annealing at 1500, 1100, and 600 °C. The XRD patterns that characterize solid solution regions in the CeO_2-Sm_2O_3 system at 1100 °C are shown in Figure 3, where the presence of two phases is distinctly seen at any percentage of components and phases, which made it possible to carry out an accurate phase analysis.

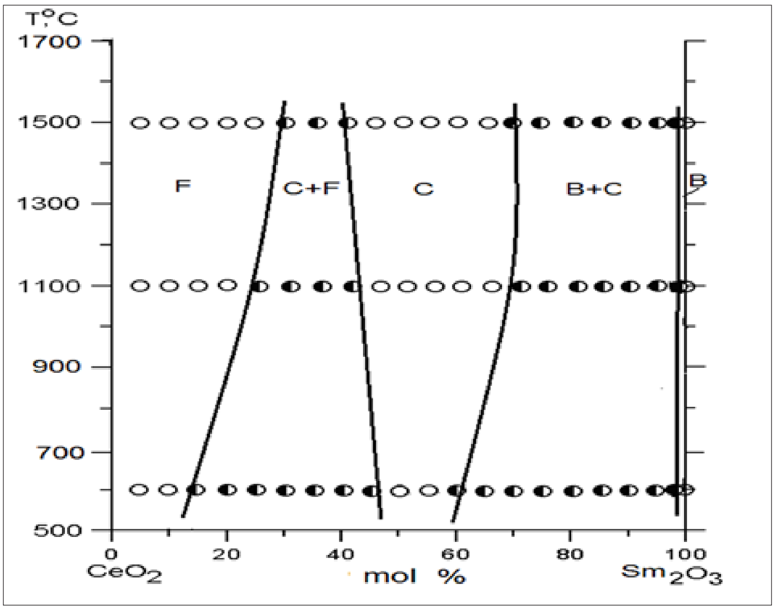

Figure 1: Phase equilibria in the CeO2-Sm2O3 system at 1500-600 °C (○-single-phase samples, ◐-two-phase samples).

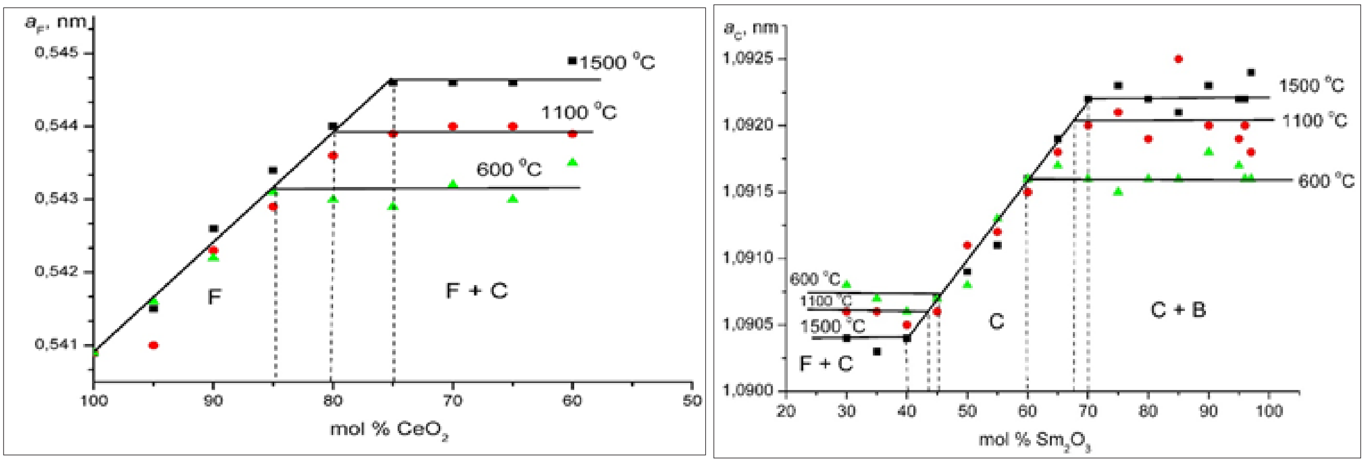

Figure 2: Concentration dependences of lattice parameters for solid solutions based on

a) F-CeO2 and

b) C- Sm2O3 in the system CeO2-Sm2O3 heat-treated at 1500 °C(■), 1100 °C (●) and 600 °C (▲).

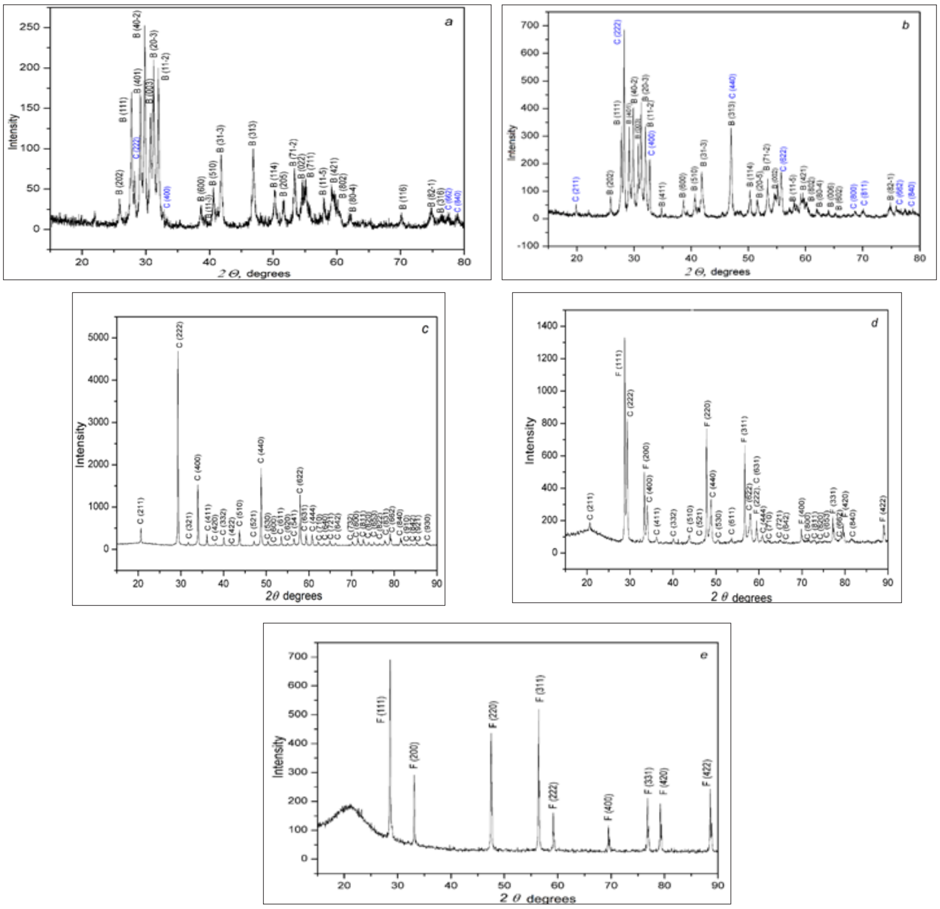

Figure 3: XRD patterns from CeO2-Sm2O3 samples annealed at 1100 °C.

(a) 1 mol.% CeO2-99 mol.% Sm2O3, (C+B)

(b) 5 mol.% CeO2-95 molл.% Sm2O3, (C+B↓)

(c) 35 mol.% CeO2-65 mol.% Sm2O3 (C)

(d) 70 mol.% CeO2-30 mol.% Sm2O3 (C+F)

(e) 95 мол.% CeO2-5 мол.% Sm2O3 (F).

Table 1: Phase composition and lattice parameters of the phases in the CeO_2-Sm_2O_3 system, annealed at 1500 °C for 150h in air (XRD data).

Chemical Composition (mol %)		Phase Composition	Lattice Parameters of the Phases a±0.0002(nm)					
CeO_2	Sm_2O_3		<F>	<C>	<B>			
			a	a	a	b	c	β
0	100	<B>	-	-	1.3925	0.3632	0.868	90.4
1	99	<B>	-	-	1.3637	0.3615	0.8928	91.7
2	98	<B>	-	-	1.3655	0.3631	0.8922	91.9
3	97	<B> + <C>	-	1.0924	1.3018	0.3578	0.9437	88.5
4	96	<B> + <C>	-	1.0922	1.3932	0.36	0.9157	91.6
5	95	<B> + <C>	-	1.0922	1.5144	0.3639	0.8095	96.9
10	90	<B> + <C>	-	1.0923	1.4629	0.3606	0.9128	87
15	85	<B> + <C>	-	1.0921	1.5763	0.3607	0.909	94.5
20	80	<B>+ <C>	-	1.0922	1.6996	0.3705	0.8518	99.1
25	75	<B> + <C>	-	1.0923	-	-	-	-
30	70	<B>+<C>	-	1.0922	-	-	-	-
35	65	<C>	-	1.0919	-	-	-	-
40	60	<C>	-	1.0916	-	-	-	-
45	55	<C>	-	1.0911	-	-	-	-
50	50	<C>	-	1.0909	-	-	-	-
55	45	<C>	-	1.0907	-	-	-	-
60	40	<C> + <F>	0.5449	1.0904	-	-	-	-
65	35	<C> + <F>	0.5446	1.0904	-	-	-	-
70	30	<C> + <F>	0.5446	1.0903	-	-	-	-
75	25	<F>	0.5446	-	-	-	-	-
80	20	<F>	0.544	-	-	-	-	-
85	15	<F>	0.5434	-	-	-	-	-
90	10	<F>	0.5426	-	-	-	-	-
95	5	<F>	0.5415	-	-	-	-	-
100	0	<F>	0.5409	-	-	-	-	-

Designation of phases: <B>-Solid solutions based on monoclinic modification of Sm_2O_3; <C>-Solid solutions based on cubic modification of Sm_2O_3; <F>-Solid solutions based on cubic modification with fluorite-type structure of CeO_2.

Table 2: Phase composition and lattice parameters of the phases in the CeO2-Sm2O3 system, annealed at 1100 °C for 10813h in air (XRD data).

Chemical Composition (mol %)		Phase Composition	Lattice Parameters of the Phases a±0.0002(nm)					
CeO_2	Sm_2O_3		<F>	<C>	<B>			
			a	a	a	b	c	β
0	100	<B>	-	-	1.3925	0.3632	0.868	90.4
1	99	<B>+<C>	-	1.0918	1.3153	0.367	0.8666	91.7
2	98	<B>+<C>	-	1.092	1.4002	0.3653	0.8721	91.9
3	97	<B>+<C>	-	1.0918	1.6469	0.3679	0.8726	88.5
4	96	<B> + <C>	-	1.092	1.7067	0.3702	0.8719	91.6
5	95	<B> + <C>	-	1.0919	1.4041	0.3398	0.8718	96.9
15	85	<B> + <C>	-	1.0925	1.6291	0.3667	0.8734	94.5
20	80	<B> + <C>	-	1.0919	1.3113	0.3612	0.918	99.1

25	75	<B> + <C>	-	1.0921	-	-	-	-
30	70	<B> + <C>	-	1.092	-	-	-	-
35	65	<C>	-	1.0918	-	-	-	-
40	60	<C>	-	1.0915	-	-	-	-
45	55	<C>	-	1.0912	-	-	-	-
50	50	<C>	-	1.0911	-	-	-	-
55	45	<C>	-	1.0906	-	-	-	-
60	40	<C> + <F>	0.5439	1.0905	-	-	-	-
65	35	<C> + <F>	0.544	1.0906	-	-	-	-
70	30	<C>+ <F>	0.544	1.906	-	-	-	-
75	25	<C>+ <F>	0.5439	-	-	-	-	-
80	20	<F>	0.5436	-	-	-	-	-
85	15	<F>	0.5429	-	-	-	-	-
90	10	<F>	0.5423	-	-	-	-	-
95	5	<F>	0.541	-	-	-	-	-
100	0	<F>	0.5409	-	-	-	-	-

Table 3: Phase composition and lattice parameters of the phases in the CeO2-Sm2O3 system, annealed at 600 °C for 33000h in air (XRD data).

Chemical Composition (mol %)		Phase Composition	Lattice Parameters of the Phases a±0.0002(nm)					
CeO_2	Sm_2O_3		<F>	<C>	<B>			
			a	a	a	b	c	β
0	100	<B>	-	-	1.3925	0.3632	0.868	90.4
1	99	<B>+<C>	-	1.0918	1.3153	0.367	0.8666	91.7
2	98	<B>+<C>	-	1.092	1.4002	0.3653	0.8721	91.9
3	97	<B>+<C>	-	1.0916	1.6469	0.3679	0.8726	88.5
4	96	<B> + <C>	-	1.0916	1.7067	0.3702	0.8719	91.6
5	95	<B> + <C>	-	1.0917	1.4041	0.3398	0.8718	96.9
10	90	<B> + <C>	-	1.0918	1.3514	0.366	0.5208	
15	85	<B> + <C>	-	1.0916	1.6291	0.3667	0.8734	94.5
20	80	<B> + <C>	-	1.0916	1.3113	0.3612	0.918	99.1
25	75	<B> + <C>	-	1.0915	-	-	-	-
30	70	<B> + <C>	-	1.0916	-	-	-	-
35	65	<B> + <C>	-	1.0917	-	-	-	-
40	60	<B> + <C>	-	1.0916	-	-	-	-
45	55	<B> + <C>	-	1.0913	-	-	-	-
50	50	<C>	-	1.0908	-	-	-	-
55	45	<C>	-	1.0907	-	-	-	-
60	40	<C> + <F>	0.5435	1.0906	-	-	-	-
65	35	<C> + <F>	0.5443	1.0907	-	-	-	-
70	30	<C>+ <F>	0.5432	1.908	-	-	-	-
75	25	<C>+ <F>	0.5429	-	-	-	-	-
80	20	<C>+ <F>	0.5443	-	-	-	-	-
85	15	<C>+ <F>	0.5431	-	-	-	-	-
90	10	<F>	0.5422	-	-	-	-	-
95	5	<F>	0.5416	-	-	-	-	-
100	0	<F>	0.5409	-	-	-	-	-

Homogeneity region boundaries of F-CeO_2 based solid solutions correspond to the following compositions: 25-30 % Sm_2O_3 at 1500 °C, 20-25 % Sm_2O_3 at 1100 °C, and 10-15 % Sm_2O_3 at 600 °C (Tables 1-3). The change in the lattice parameters in F-CeO_2 based solid solutions against the Sm_2O_3 concentration is shown in (Figure 2a). The results depicted in Figure 1 and 2 suggest that the solubility of Sm_2O_3 in F-modification of CeO_2 is about 15mol % for 600 °C and 20mol % for 1100 °C and 25mol % for 1500 °C. Lattice parameters increases from a=0.5409nm for pure CeO_2 to a=0.5446nm (1500 °C), 0.5436nm (1100 °C), and 0.5422nm (600 °C) for the limit solid solution compositions.

Dissolution of samaria in ceria during annealing in air proceeds by mutual diffusion and solid solution formation through different-valence substitution: Sm^{3+} ions substitute for Ce^{4+} ions in the F-type lattice sites. In order to preserve charge neutrality of the crystal, the difference in ion charge is compensated by the appearance of oxygen vacancies in sites of oxygen ions. There are however such solubility limit values which correspond to a critical concentration of vacancies, beyond of which the fluorite-type (Fm3m) lattice becomes unstable and transforms into another cubic lattice, namely IA_3, characteristic for solid solutions of the C-type on the basis of REE oxides. The solubility limit increases with temperature rising.

Homogeneity region boundaries of C-Sm_2O_3 based solid solutions correspond to the following compositions: 45-65 % Sm_2O_3 at 1500 and 1100 °C, and 45-50 % Sm_2O_3 at 600 °C (Tables 1-3). The parameter of the unit cell C phase increases from a=1.0904nm in the two-phase sample (F+C) containing 40mol % Sm_2O_3 to a=1.0922nm in the two-phase sample (B+C) containing 70mol % Sm_2O_3 (at 1500 °C Table 1) and from a=1.0905nm in the two-phase sample (F+C) containing 40mol % Sm_2O_3 to a=1.0915nm in the two-phase sample (B+C) containing 70mol % Sm_2O_3 (at 1100 °C Table 2) and from a=1.0906nm in the two-phase sample (F+C) containing 40mol % Sm_2O_3 to a=1.0913nm in the two-phase sample (B+C) containing 55mol % Sm_2O_3 (at 600 °C Table 3).

The spread of the homogeneity field of the solid solution based on B-Sm_2O_3 at 600, 1100 °C remains negligible, less than 1 mol % and 3 mol % for 1500 °C. The substitution of ions Sm^{3+} (r=0.100nm) in the lattice of Sm_2O_3 by smaller ions Ce^{4+} (r=0.090nm) does not result in stabilization of the B-Sm_2O_3 neither at 600, nor at 1100 °C. Lattice parameters increases from a=1.3925nm, b=0.3632nm, c=0.8680nm, β=90.4 for pure Sm_2O_3 to a=1.3018nm, b=0.3578nm, c=0.9433nm, β=88.5 in the two-phase sample (B+C) containing 97mol % Sm_2O_3 (1500 °C) and to a=1.3153nm, b=0.3670nm, c=0.8666nm, β=91.7 in the two-phase sample (B+C) containing 99mol % Sm_2O_3 (1100 and 600 °C). XRD patterns acquired from in the CeO_2-Sm_2O_3 system at 1100 °C are presented in Figure 3a. As seen, at 1100 °C, the sample 1mol % CeO_2-99mol % Sm_2O_3, in addition to the basic B-phase, exhibits distinct peaks which are characteristic for the cubic C-phase.

The results obtained may be interpreted on the basis of literature data [19,14], which will permit one to forecast phase interaction and properties of solid solutions in other systems of the CeO_2-Ln_2O_3 series. The 25mol % Eu_2O_3 doped CeO_2 preserves the initial F-type of the CeO_2 lattice (1500 °C). Thus, a decrease in the lanthanide ion radius makes the homogeneity region of F-CeO_2 based solid solutions narrower: from 49mol % for La^{3+} (0.104nm) [19,14] to 25mol % for Sm^{3+} (0.100nm) (this work) at 1500 °C and from 49mol % for La^{3+} (0.104nm) [19] to 20mol % for Sm^{3+} (0.100nm) (this work) at 1100 °C.

Conclusion

The phase equilibria in the CeO_2-Sm_2O_3 system at 600, 1100 and 1500 °C were studied in the whole concentration range. The subsection of the phase diagram has been developed. The solid solutions of monoclinic (B) modification of Sm_2O_3, and cubic (C) modification of Sm_2O_3 with C-type structure of rare-earth oxides, as well as solid solution with cubic modification of CeO_2 with fluorite-type structure (F) were found that had limited solubility. The refined solubility of Sm_2O_3 in cubic F-ceria decreases from 25 to ~15mol % with decreasing temperature at 1500 and 600 °C, respectively. The width of the homogeneity field of the solid solutions based on B-Sm_2O_3 is less than 1mol % at 600-1100 °C and 3 mol % for 1500 °C. In this temperature range, ordering of intermediate phases was not confirmed.

References

[1] Zhu D, Miller R (2004) Development of advanced low conductivity thermal barrier coatings. Int J Appl Ceram Technol 1(1): 86-94.

[2] Dudek M, Mroz ŁM, Drożdż-Cieŝla E (2008) Synthesis of ceria-based nanopowders suitable for manufacturing solid oxide electrolytes. Materials Science-Poland 26(2): 319-329.

[3] Dudek M (2013) Some structural aspects of conductivity in co-doped ceria based electrolytes. Archives of Metallurgy and Materials 58(4): 1355-1359.

[4] Sudarsanam P, Kuntaiah K, Reddy BM (2014) Promising ceria-samaria-based nano-oxides for low temperature soot oxidation: A combined study of structure-activity properties. New J Chem 38(12): 5991-6001.

[5] Reis SL, Carvalho SGM, Muccillo ENS, Muccillo R (2019) Electrical behavior of electric field-assisted pressureless sintered ceria-20 mol% Samaria. Ceramics 2: 385-392.

[6] Pinheiro D, Devi KRS, Karthik K, Jose A, Sugunan S (2019) Phytogenic CeO_2-Sm_2O_3 nanocomposites with enhanced catalytic activity for reduction of 4-nitrophenol. Mater Res Express 6(8): 084011.

[7] Rangaswamy A, Sudarsanam P, Reddy BM (2015) Rare earth metal doped CeO_2-based catalytic materials for diesel soot oxidation at lower temperatures. Journal of Rare Earths 33(11): 1162-1169.

[8] Coduri M, Masala P, Allieta M, Peral I, Brunelli M, et al. (2018) Phase transformations in the CeO_2-Sm_2O_3 System: A multiscale powder diffraction investigation. Inorg Chem 57(2): 879-891.

[9] Kharissova AB, Hinojosa Rivera M, Kharissova OV (2018) Synthesis and characterization of CeO_2 doped with Sm_2O_3 and Eu_2O_3 for the use in SOFCs. MRS Advances 3(32): 1855-1861.

[10] Maguire E, Gharbage B, Marques FMB, Labrincha JA (2000) Cathode materials for intermediate temperature SOFCs. Solid State Ionics 127(3-4): 329-335.

[11] Andrievskaya ER, Kornienko OA, Bykov OI, Sameliuk AV, Bohatyriova ZD (2019) Interaction of ceria and ytterbia in air within temperature range 1500-600 °C. Journal of the European Ceramic Society 39(9): 2930-2935.

[12] Andrievskaya ER, Kornienko OA, Sameljuk AV, Sayir A (2020) Phase relation studies in the CeO_2-Eu_2O_3 system at 600 to 1500 °C in air. Journal of the European Ceramic Society 40(3): 751-758.

[13] Toropov SA (1987) Phase diagrams of the refractory oxide systems, binary systems. chapter 3, Leningrad, Nauka 5: 264.

[14] Andrievskaya ER, Kornienko OA, Ali Sayir, Vasylkiv OO, Sakka Y (2011) Phase relation studies in the ZrO_2-CeO_2-La_2O_3 system at 1500 °C Journal of the American Ceramic Society 94(6): 1911-1919.

[15] Kornienko OA (2009) Interaction and phase properties in the CeO_2-Gd_2O_3 system at 1500 °C. 45: 86-90.

[16] Mandal BP, Grover V, Tyagi AK (2006) Phase relations, lattice thermal expansion in $Ce_{1-x}Eu_xO_{2-x/2}$ and $Ce_{1-x}Sm_xO_{2-x/2}$ systems and stabilization of cubic RE_2O_3 (RE: Eu, Sm). Materials Science and Engineering: A 430(1-2): 120-124.

[17] Grover V, Banerji A, Sengupt P, Tyagi AK (2008) Raman, XRD and microscopic investigations on CeO_2-Lu_2O_3 and CeO_2-Sc_2O_3 systems: A sub-solidus phase evolution study. Journal of Solid State Chemistry 181(8): 1930-1935.

[18] Andrievskaya ER (2008) Phase equilibria in the refractory oxide systems of zirconia, hafnia and yttria with rare-earth oxides. Journal of the European Ceramic Society 28(12): 2363-2388.

[19] Andrievskaya ER, Kornienko OA, Sameljuk AV, Sayir A (2011) Phase relation studies in the CeO_2-La_2O_3 system at 1100-1500 °C. J of the Europ Ceram Soc 31(7): 1277-1283.